

UNIVERSIDADE DE SÃO PAULO

# PUBLICAÇÕES

INSTITUTO DE FÍSICA  
CAIXA POSTAL 20516  
01452-990 SÃO PAULO - SP  
BRASIL

IFUSP/P-1128    SYSNO: 874221

**PULSED NUCLEAR QUADRUPOLE RESONANCE  
IN NON-UNIFORMLY DISORDERED SYSTEMS**

**Said R. Rabbani, N. Caticha and João G. dos Santos**  
Instituto de Física Universidade de São Paulo

**Daniel J. Pusiol**  
FAMAP, Universidad Nacional de Córdoba,  
Medina Allende y Haya de la Torre, 5000 Córdoba, Argentina

Outubro/1994

## Pulsed nuclear quadrupole resonance in non-uniformly disordered systems

Said R. Rabbani, N. Caticha and João G. dos Santos  
Instituto de Física, Universidade de São Paulo, Caixa Postal 20516,  
01498-970, São Paulo, SP, Brazil

Daniel J. Pusiol  
FAMAF, Universidad Nacional de Córdoba, Medina Allende y Haya de la  
Torre, 5000 Córdoba, Argentina

October 21, 1994

**Running title:**  
NQR in crystalline and disordered phases

### Abstract

Pulsed nuclear quadrupole resonance (NQR) measurements, at room temperature and 77 K have been performed on distinct specimen of arsenolite (a) polycrystalline sample and (b) in a specimen with a varying degree of disorder, ranging from amorphous to crystalline order. The NQR absorption line in these specimen, obtained by the fast Fourier transform (FFT) method, has different intensity and line-shape. A theoretical model is proposed which explains the experimental results very well. The model is based on the assumption that the electric field gradient (EFG), due to the intermolecular interaction, changes randomly from site to site characterized by a distribution. In sample (b) this distribution is approximately constant in regions of mesoscopic dimensions ( i.e. large enough to have few hundred interatomic distances but small enough compared to the bulk dimensions of the sample ) but changes throughout the sample. The scanning electron micrographs of these samples are presented which support our assumption.

## 1 Introduction

Arsenic compounds are common in different materials like crystals, amorphous semiconductors, glasses, super lattices, etc. Due to the importance of and the ease in observing the nuclear quadrupole resonance (NQR) of  $^{75}\text{As}$ , the NQR studies of this nucleus has been reported in a variety of compounds like elemental arsenic, arsenic sulfide, arsenic telluride, arsenic selenide in crystalline and vitreous forms [1, 2, 3]. In the late seventies and early eighties some articles were presented discussing the structure of  $\text{As}_2\text{O}_3$  in crystalline and vitreous state [4, 5, 6, 7, 8]. Few others were presented studying this material by means of the NQR, demonstrating the power of this technique to analyze short range order properties [9, 10, 11, 12]. NQR of different nuclei has been used to study glasses and the theoretical model has been presented to describe the NQR line shape of organic glasses [13]. A common feature in these NQR works is that the samples used are either polycrystalline or amorphous, where the disorder is uniform throughout the sample. As far as we know, this is the first work which deals with a specimen where the electric field gradient (EFG) due to the intermolecular interaction changes randomly from site to site characterized by a distribution which varies in different regions of the sample.

Crystals containing NQR sensitive nuclei were used as filler material in polymers, to study the internal stress induced by the polymerization of copolymers [14]. A theoretical work with some experimental data in uniaxial-

stress dependence of the NQR frequency was done by Zamar et.al [15]. Arsenolite ( $\text{As}_2\text{O}_3$ ) and senarmonite ( $\text{Sb}_2\text{O}_3$ ) are good candidates to be used as probes for local stress distribution. The commercial powder of arsenolite, the high temperature stable phase of  $\text{As}_2\text{O}_3$ , has been used to test the NQR imaging in the rotating frame method [16, 17, 18]. The spatial resolution of the image and the sensitivity of the technique strongly depend on the NQR line shape and intensity respectively. The narrower the lines are, the higher is the spatial resolution and the more intense the lines are, the higher is the sensitivity of the method. The results presented in this paper shows that the polycrystalline samples obtained from the commercial powder by a recrystallization process are much more suitable for these studies.

## 2 Experimental

The measurements were performed using an automatized home made NQR spectrometer which was built using the following equipment: a Matec gating modulator (Mod. 5100), a Matec broad band receiver (Mod. 625) and a Phillips Frequency Synthesizer (Mod. PM5390S). The data acquisition system is composed of a Tektronix digital oscilloscope (Mod. 2430A), and IBM compatible AT 286 microcomputer and a Hewlett-Packard measurement plotting system (Mod. 7090A). A commercial Asyst program, specially configured for this experiment, was used for transferring and analyzing the data. The powder samples of  $\text{As}_2\text{O}_3$  (PW), with grains of approximately

10-100  $\mu\text{m}$  were obtained from Merck Company and used without further purification. The finer powder (FP) of material was obtained by grinding the commercial powder, however the size of the grains were not determined. The polycrystalline sample (PL) was prepared by slow evaporation at 50  $^{\circ}\text{C}$  in an oven from a saturated and filtered aqueous solution of  $\text{As}_2\text{O}_3$ . An additional set of samples was prepared and annealed at 250  $^{\circ}\text{C}$  during 20 hours. In the NQR spectra of these material no line due to claudetite was present, which shows that during the annealing process no arsenolite to claudetite phase transition had happened. Due to the toxic nature of  $\text{As}_2\text{O}_3$ , extra care should be taken during the preparation and handling of samples. The NQR spectra was obtained from spin echo by Fast Fourier Transform (FFT) algorithm. The scanning electron micro graphs of the powder samples were obtained by stereoscan 180 (Cambridge) and those of polycrystalline samples by Jeol JEM 840-A.

### 3 Results

#### 3.1 NQR line shape

Some typical NQR spectra of PW, FP and PL samples with and without annealing are presented in this section. Fig. 1 shows the NQR absorption line of polycrystalline sample (PL), at room and liquid nitrogen temperature. In both cases the spectral line can be fitted to a single gaussian with the full width at half maximum (FWHM) 5.37 KHz and 6.25 KHz respectively. This

is a clear indication that the sample is polycrystalline. This fact is confirmed by the micro graphs presented in fig 5.

#### INSERT FIGURE 1

Fig. 2 depicts the same as Fig. 1 for commercial powder (PW). In this sample NQR line is broader and cannot be fitted with a single gaussian or lorentzian, demonstrating that the spread in EFG is not constant throughout the sample.

#### INSERT FIGURE 2

The corresponding NQR spectrum of FP sample at room temperature is shown in Fig. 3a. Again the NQR line in this sample is broader than that of PL and PW samples and cannot be fitted neither by a single gaussian nor lorentzian.

#### INSERT FIGURE 3

The broadening of the NQR line in respect to the PW sample is due to the internal stress induced during the mechanical treatment. After annealing process the NQR line of the FP sample has a similar line width to the PW sample, which shows the stress relaxation during the heat treatment Fig 3b. The heat treatment does not have any considerable influence on PL and PW samples.

### 3.2 Scanning electron micro graph

The scanning electron micro graphs of PW sample with amplification factors of 132, 792 and 2500 are shown in Fig. 4a, b and c respectively. As overview of PW sample reveals (Fig. 4a), the granulate material is composed of about  $100 \mu m$  almost spherical grains. One of the unbroken grains is shown in Fig. 4b. Fig. 4c presents the detail of a broken grain. A polycrystalline structure is observed in the inner part of the grain, resembling the arsenolite crystalline structure, however, the shell material seems to be amorphous.

INSERT FIGURE 4

The micro graphs corresponding to the PL sample with amplification factors of 44, 125 and 1250 are presented in Figs. 5a, b and c respectively. As it can be seen, this material is made of different size monocrystals and there is no evidence of amorphous parts.

INSERT FIGURE 5

### 3.3 Integrated spin-echo intensity

It is well known that amorphous arsenolite has a much broader NQR absorption line than the polycrystalline one [10]. Therefore, in order to

compute the fraction of material in PW sample which is narrow enough to be detected, we compared the area covered by the spin echo of 200 mg of PW and PL samples. The experimental condition was checked by measuring the PW and PL spin-echo intensity in a PW, PL, PW sequence by changing the sample without any change in spectrometer adjustment. No appreciable change on the signals of each sample was observed in the sequence. The Area PW/Area PL ratio was .55, in other words, only 55% of commercial powder is detectable. Another 45% is too broad to be detected. It is reasonable to assume that the NQR line in PW is progressively broadened from center to the border of the grains and eventually becomes so broadened that it is not detectable any more.

## 4 Theory

The effect of disorder in the line shape of the NQR spectrum has been the subject of previous studies [13]. The aim of this work is to study both theoretically and experimentally this effect in a more general setting, where the disorder is not uniform, but varies throughout the sample.

Due to the dependence of the resonance frequency on the EFG, the disorder will influence the resonance frequency in a manner which reflects the local distribution of disorder. Consider a generalized random displacement field  $u$ . The resonance frequency in a region can be thought, barring extreme cases, as an analytical function of  $u$  and can thus be expanded in a Taylor

series

$$\nu = \nu_0 + a_1 u + \frac{a_2}{2} u^2 + \dots \quad (1)$$

The actual value of the derivatives of  $\nu$  w.r.t  $u$  is not known, for its theoretical calculation is beyond present approximation schemes. As has been done before [13], this lack of knowledge leads to the treatment of  $a_i$  as fitting parameters.

The model of the disorder we have in mind is as follows. On an intermolecular scale,  $u$  varies randomly from site to site characterized by a distribution. This distribution is the same inside a certain region of mesoscopic dimensions  $(\Delta r)^3$ , i.e. large enough to have few hundred interatomic distances but small compared to the bulk dimensions of the sample.

It is natural to assume that  $u$  is described by  $f_r(u)$ , a gaussian distribution which we take to be

$$f_r(u) = \frac{1}{\sqrt{2\pi}\sigma_r} e^{-\frac{u^2}{2\sigma_r^2}} \quad (2)$$

and the width of the distribution may vary on a mesoscopic length scale.

Due to equation 2 it can be seen that the contribution of a given region  $(\Delta r)^3$  will be

$$\rho_r(\nu) d\nu = f(u_r) du_r \quad (3)$$

thus

$$\rho_r(\nu) = \frac{f(u_r)}{\left| \frac{d\nu}{du_r} \right|} \quad (4)$$

the total spectral density will be the incoherent sum of all such contributions

from the sample:

$$\rho(\nu) = \int_{\text{sample}} \rho_r(\nu) \frac{d^3 r}{V} \quad (5)$$

where the integral is over the sample of volume  $V$ . This is quite general and we now look at the particular case where the material, as described in section 3, is a powder which according to the experimental data, has a crystalline order at the center and is rather amorphous at the surface of almost spherical powder particles.

The basic point of the following analysis is to argue that the width of  $f_r(u)$  grows as one goes from the center to the surface of the sphere. For the polycrystalline sample this is not true and the crystallization is more or less constant throughout the sample, as can be seen in the electron micrographs of fig 5 and the gaussian shape of the NQR line of fig 1. We model the width  $\sigma(r)$  of the distribution by a homogeneous function of  $r$ . The important feature is its growth and not the specific details of its variation. For simplicity and because it is not necessary to put more details than necessary to explain the experimental data, we take  $\sigma(r)$  to be linear in  $r$  and assume spherical symmetry,

$$\sigma(r) = br. \quad (6)$$

The value of  $b$  is not known and it will turn out not to be important. With this simplification the spectral density is given by

$$\rho(\nu) = \frac{3}{\sqrt{2\pi} R_0^3 \left| \frac{d\nu}{du} \right|} \int_0^{R_0} \left( e^{-\frac{1}{2} \frac{\nu^2}{b^2 r^2}} \right) \frac{r dr}{b} \quad (7)$$

where  $R_0$  is the radius of the sphere. By defining a new rescaled integration variable  $\frac{br}{u} = x$  and calling  $\frac{bR_0}{u} = \frac{1}{y}$ , we have

$$\rho(\nu) = \frac{3}{\sqrt{2\pi} \left| \frac{dv}{dy} \right|} y^2 \int_0^{\frac{1}{y}} e^{-\frac{1}{2x^2}} x dx \quad (8)$$

In this form we have rescaled the generalized displacement field  $u$  and substituted by  $y$ . Equation 1 can be rewritten as

$$\nu = \nu_0 + \tilde{a}_1 y + \frac{\tilde{a}_2}{2} y^2 + \dots \quad (9)$$

Where  $\tilde{a}_1$  and  $\tilde{a}_2$  are related to the previously unknown  $a_1$  and  $a_2$  by

$$\tilde{a}_1 = a_1 b R_0 \quad , \quad \tilde{a}_2 = a_2 (b R_0)^2 \quad (10)$$

Notice the important fact that all new unknown parameters that were introduced in the modelling process have not implied in a larger number of fitting parameters. The line shape is thus described by a prefactor, which carries basic quadrupolar influences, times a universal function  $F(y)$  given by

$$F(y) = y^2 \int_0^{\frac{1}{y}} e^{-\frac{1}{2x^2}} x dx \quad (11)$$

The only parameters to be fitted are  $\tilde{a}_1$ ,  $\tilde{a}_2$  and the ordered state resonance frequency  $\nu_0$ .

As reported in [13] the effect of a non zero  $\tilde{a}_2$  is to introduce asymmetry with respect to  $\nu_0$ . In the case of the material we study, the symmetrical line shape strongly indicates that the effect of  $\tilde{a}_2$  is negligible and thus can be taken as zero. We are left with a one parameter fit. The excellent agreement with the experimental data is discussed in the next section.

## 5 Discussion

Before attempting to compare equation 8 with the experimental results we should mention several points.

a) As it can be seen in fig 4 the grains of the powder are neither spherical nor uniform in size, varying almost an order of magnitude in diameter.

b) In developing the theory it was assumed that the disorder starts at the center and goes all the way to the surface. However, it is perfectly possible that there is a central part of the grains which maintain the crystalline order and contribute to the line shape with a gaussian of constant line width. This would change slightly the line shape.

With the above considerations it is clear that the theory presented is an order of magnitude calculation and the general shape of the spectrum is the best test for the theory rather than the values of the parameters derived from it. However, it should be mentioned that the theory can be used for more quantitative analysis when the disorder profile is known.

A careful search was carried out from 90 MHz to 117 MHz within the temperature range of 77 K to 300 K. The only absorption line detected was the one corresponding to arsenolite around 116 MHz. In particular, no signal from claudetite was found. The experimental data of Figure 1a and 1b can be well fitted to a single gaussian. Therefore, it is reasonable to assume that the polycrystalline arsenolite has a gaussian shape NQR line with a line width of approximately 5 KHz. The NQR lines corresponding to PW and FP are

neither a pure gaussian nor lorentzian and are broadened compared to PL sample, figure 2 and 3. In the case of FP sample the NQR line is broader than the PW line, however, after the annealing process its line width is comparable to the PW line width and the annealing process does not have any appreciable effect on PL and PW samples.

Since we could not find any extra lines in the PW sample, it is clear that the 45% reduction in NQR signal in this sample is due to the broadening of NQR line in some region of the sample, making the signal from this region undetectable. Furthermore, the annealing process does not show any appreciable effect on the NQR line of PW sample which indicates that the broadening is due to structural disorder and not to any mechanical stress. Therefore, it justifies to use the equation 8 to fit our experimental data. As it can be seen in figures 2 and 3, the theoretical curves (solid line) fit very well the experimental data (solid circles). These confirm our assumption that the line width of NQR line changes from region to region of the sample.

A series of works [16. 19. 17. 20] have been done using  $As_2O_3$  as a probe to measure the stress effect in polymers and for imaging purposes. In these works the commercial powder of  $As_2O_3$  were used, however our results show that a recrystallized material would render much better result, increasing the sensitivity and the resolution of these techniques.

## 6 Acknowledgements

The Authors thank the National Research Councils of Brazil and Argentina (CNPq and CONICET, respectively) for the financial support in the form of the joint research agreement and through the award of research fellowships.

The scanning electron micro graphs were kindly taken by Dr. Pedro K. Kiyohara of the Laboratório de Microscopia Eletrônica do Instituto de Física da Universidade de São Paulo. One of us (DJP) acknowledges the Fundación Antorchas (Argentina) and the Córdoba Provincial Research Council (CONICOR) for Research Grants.



## References

- [1] M.Rubinstein and P.C.Taylor. *Phys. Rev. Lett.*, 29:119, 1972.
- [2] M.Rubinstein and P.C.Taylor. *Phys. Rev.*, 9B:4258, 1974.
- [3] G.E.Jellison Jr, G.L.Petersen, and P.C.Taylor. *Phys. Rev.*, 22B:3903, 1980.
- [4] R.F.Pettifer and P.W.McMillan. *Philosophical Magazine*, 35:871, 1977.
- [5] S.J.Gurman and R.F.Pettifer. *Philosophical Magazine*, 40:345, 1979.
- [6] G.Lucovsky and F.L.Galeener. *J.Non-Cryst. Solids*, 37:53, 1980.
- [7] M.Imaoka and Hasegawa. *Phys. Chem. of Glasses*, 21:67, 1979.
- [8] W.M.Pontuschka and P.C.Taylor. *Solid State Communications*, 38:573, 1981.
- [9] D.J.Treacy and P.C.Taylor. *Solid State Communication*, 40:135, 1981.
- [10] P.C.Taylor, U.Strom, W.M.Pontuschka, and D.J.Treacy. *J. Phys.Soc. Japan*, 49(Suppl. A):1155, 1980.
- [11] R.G.Barnes and P.J.Bray. *J. Chem. Phys.*, 23:1177, 1955.
- [12] P.J.Bray, R.G.Barnes, and J.G.O'Keefe. *J. Chem. Phys.*, 25:792, 1956.
- [13] A.E.Wolfenson, A.H.Brunetti, D.J.Pusiol, and W.M.Pontuschka. *Phys. Rev.*, 41B:6257, 1990.
- [14] R.R.Hewitt and B.Mazelsky. *J.Appl.Phys.*, 43:3386, 1972.
- [15] R.C.Zamar and A.H.Brunetti. *Phys. Stat. Sol. (b)*, 150:245, 1988.
- [16] R.Kimmich, E.Rommel, P.Nickel, and D.Pusiol. *Z. Naturforsch.*, 47A:361, 1992.
- [17] E.Rommel, R.Kimmich, H.Robert, and D.Pusiol. *Meas. Sci. Technol.*, 3:446, 1992.
- [18] G.S.Harbison, A.Slokenbergs, and T.M.Barbara. *J. Chem. Phys.*, 90:5292, 1989.
- [19] E.Rommel, D.Pusiol, P.Nickel, and R.Kimmich. *Meas. Sci. Technol.*, 2:866, 1991.
- [20] P.Nickel, E.Rommel, R.Kimmich, and D.Pusiol. *Chem. Phys. Lett.*, 183:183, 1991.

## FIGURE CAPTIONS

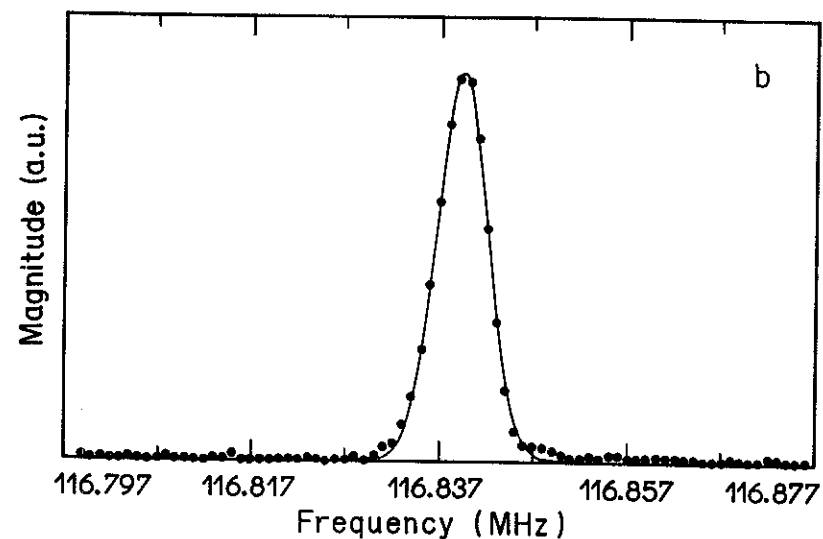
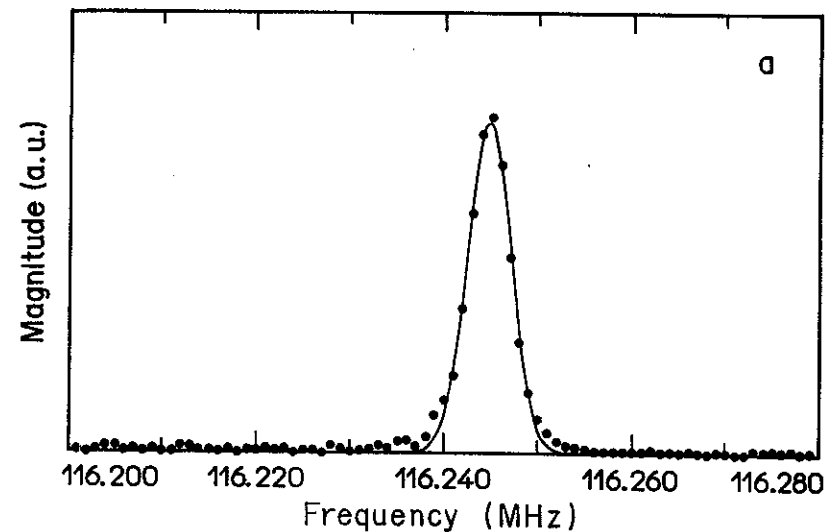
Fig. 1 NQR absorption line of polycrystalline sample (PL) at a) 300 K and b) 77 K. The experimental data (solid circles) are superimposed with a single gaussian line (solid line).

Fig. 2 NQR absorption line of commercial powder (PW) at a) 300 K and b) 77 K. The experimental data (solid circles) are superimposed with a theoretical curve (solid line) generated using the equation 8.

Fig. 3 NQR absorption line of fine powder (FP) a) without annealing at 300 K and b) annealed one at 77 K. The experimental data (solid circles) are superimposed with a theoretical curve (solid line) generated using the equation 8.

Fig. 4 The scanning electron micro graphs of PW sample with amplification factors of a) 132, b) 792 and c) 2500.

Fig. 5 The scanning electron micro graphs of PL sample with amplification factors of a) 44, b) 125 and c) 1250.



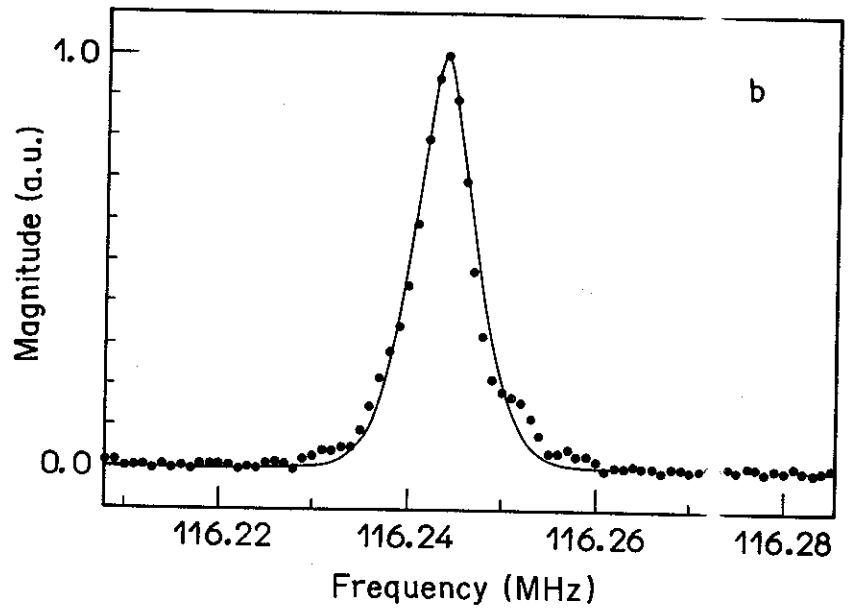
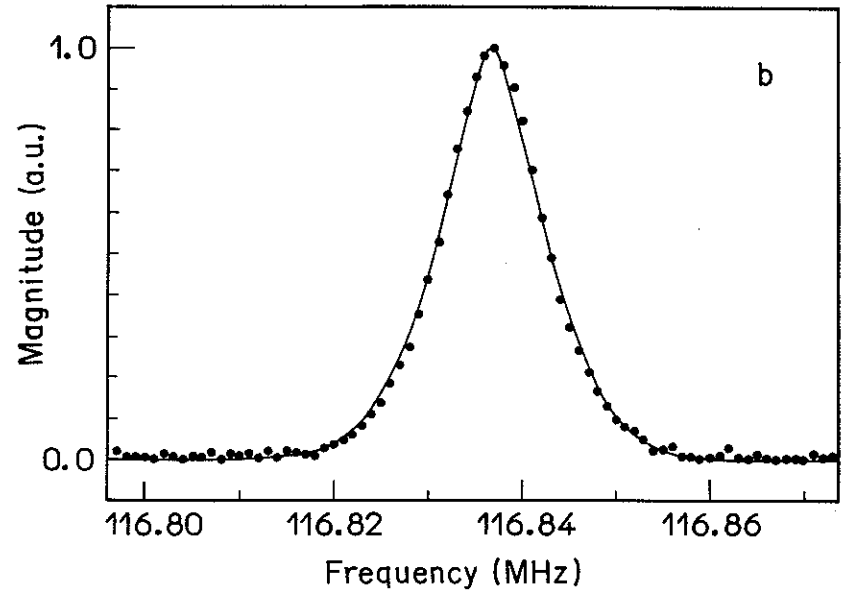
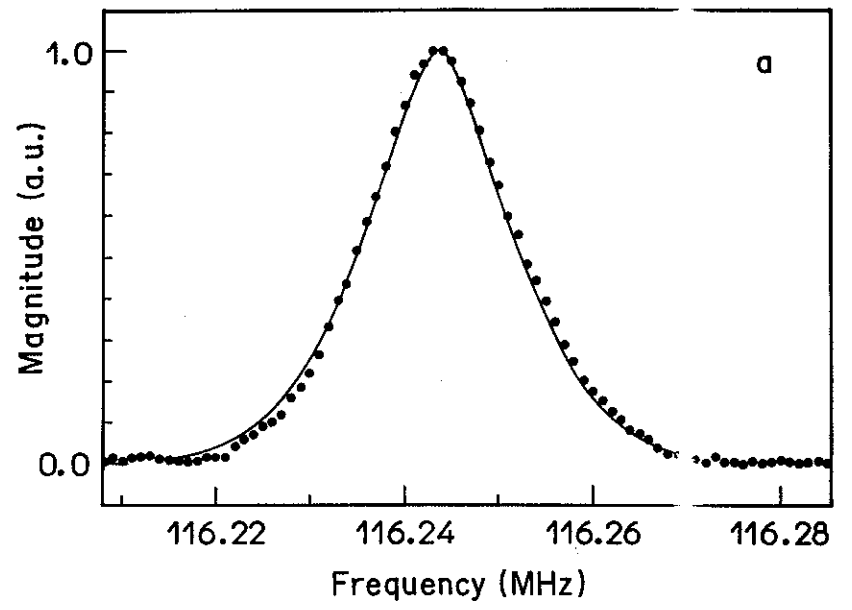
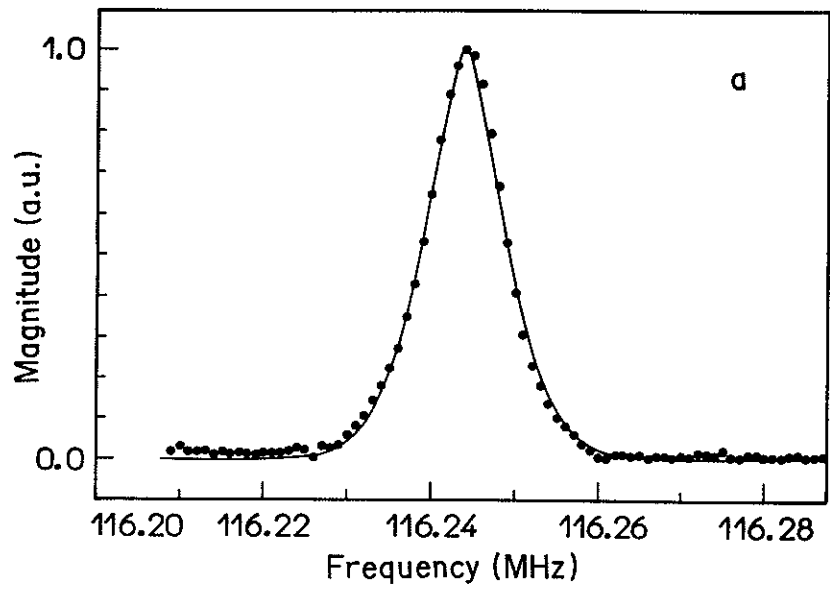


Figure 2

re 3

David F. Rehman et al. *Physical Nuclear Geochronology* ... R. Reibman et al. *Pulsed nuclear magnetic resonance*

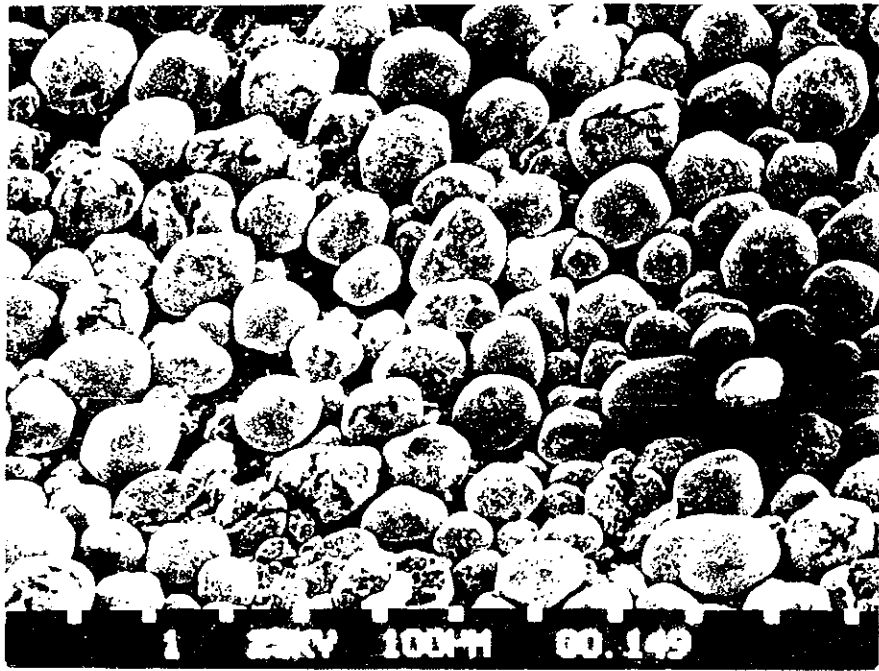


Fig. 4a  
Said R. Rabbani et.al. "Pulsed Nuclear Quadrupole ..."

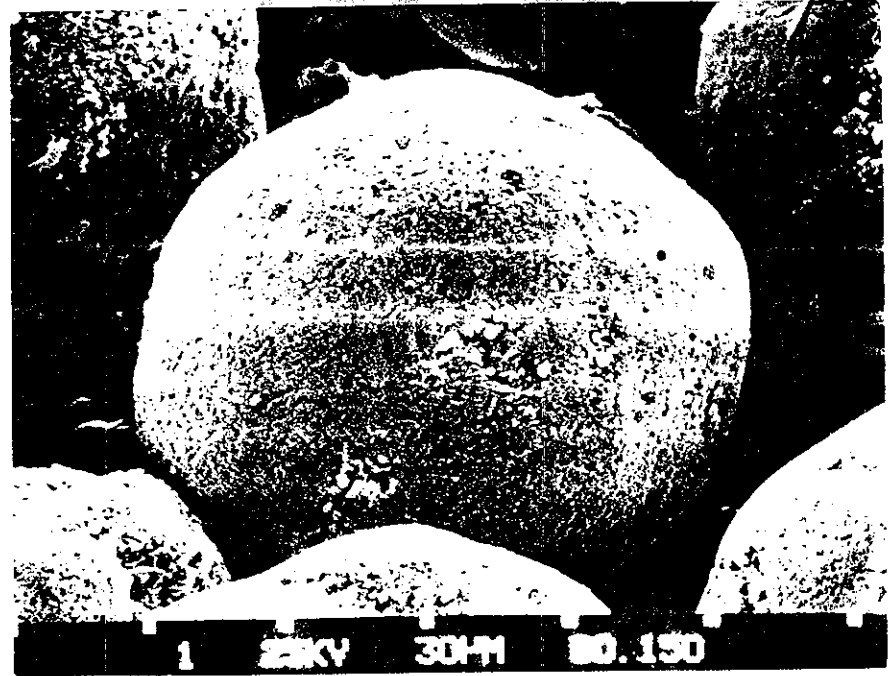


Fig. 4b  
Said R. Rabbani et.al. "Pulsed Nuclear Quadrupole ..."

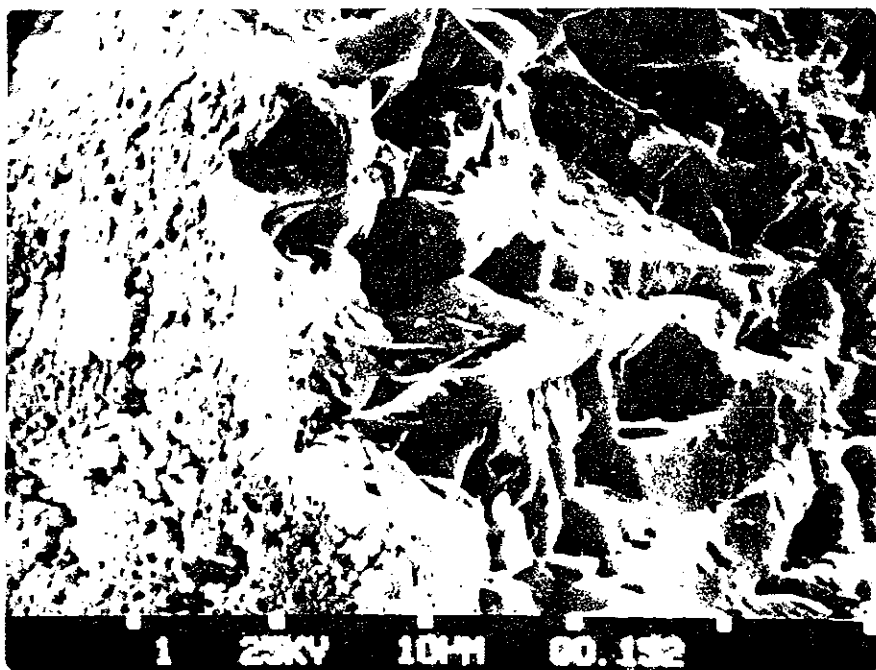


Fig. 4:  
Said R. Rabbani et.al. "Pulsed Nuclear Quadrupole ..."

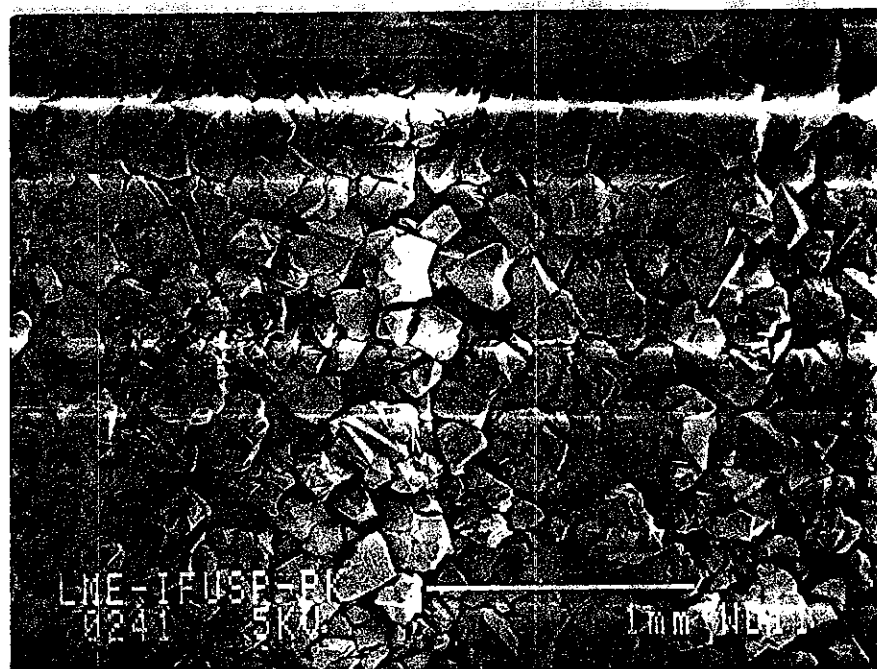


Fig. 5a  
Said R. Rabbani et.al. "Pulsed Nuclear Quadrupole ..."



Fig. 5b  
Said R. Rabbani et.al. "Pulsed Nuclear Quadrupole ..."



Fig. 5c  
Said R. Rabbani et.al. "Pulsed Nuclear Quadrupole ..."